An interference-matched notch filter for narrowband RFI suppression in SAR

Tran Van Anh[1*], Vu Tuan Anh[2], Nguyen Tien Phat[3]

[1]Institute of Defence Equipment, Academy of Military Science and Technology, 17 Hoang Sam, Nghia Do, Hanoi, Vietnam;
[2]Academy of Military Science and Technology, 17 Hoang Sam, Nghia Do, Hanoi, Vietnam;
[3]Le Quy Don Technical University, 236 Hoang Quoc Viet, Nghia Do, Hanoi, Vietnam.
[*]Corresponding author: anhstran87@gmail.com

Received 01 Jun. 2026; Revised 21 Jul. 2026; Accepted 10 Aug. 2026; Published 25 Aug. 2026.
DOI: https://doi.org/10.54939/1859-1043.j.mst.113.2026.12-19

ABSTRACT

Narrowband radio-frequency interference (NBI) degrades synthetic aperture radar (SAR) images. Frequency-domain notch filtering is a common countermeasure, but a hard (rectangular) notch trades interference rejection against raised sidelobes, and a fixed apodized (tapered) notch cannot suit emitters of different bandwidth. This paper presents a simple, low-complexity notch whose shape is matched to the measured interference spectrum. Based on the classical Wiener idea, it estimates each emitter's power spectral density from the averaged SAR range spectrum and applies a parametric minimum-mean-square-error gain whose roll-off follows that emitter; the filter is linear, needs no per-scene tuning, and costs about one spectral multiplication per pulse. On a 2-D SAR simulation with emitters of differing bandwidth it gives the lowest point-target peak sidelobe ratio (PSLR; about −15.1 dB), integrated sidelobe ratio (ISLR; about −7.2 dB) and image normalised mean-square error (NMSE; about −7.0 dB) among a hard notch and a fixed apodized notch. The contribution of this paper lies in the per-emitter spectrum-matched notch design and the comparative evaluation of the proposed method's effectiveness against other approaches.

Keywords: SAR; Radar DSP; RFI suppression; Narrowband RFI; Notch filter.

1. INTRODUCTION

Synthetic aperture radar (SAR) in the lower microwave bands increasingly shares its spectrum with terrestrial radars and communication links. The resulting radio-frequency interference (RFI) couples into the receiver and, after compression, can appear as bright streaks, ghost targets, and a raised noise floor [1]. Narrowband interference (NBI) — energy concentrated in a small part of the chirp bandwidth — is one of the more common types and is the focus of this work.

A range of mitigation methods has been studied, including eigensubspace and independent-subspace techniques [2, 3], low-rank/sparse decompositions [4], linear prediction [14], consecutive-mean excision [15], and learning-based approaches. In practical processing, frequency-domain notch filtering remains popular for NBI because it is fast and robust to the number of emitters: the contaminated range-frequency bins are detected and then attenuated. More broadly, recent Journal of Military Science and Technology (JMST) work formulated RF-interference mitigation as a two-stage time–frequency segmentation and signal-reconstruction problem and demonstrated effective recovery under broadband burst interference [16].

The hard (rectangular) notch, however, ties interference rejection to image quality. Setting a band of bins abruptly to zero is equivalent to subtracting a slowly decaying response from the impulse response; to cover an emitter's spectral skirts the notch must be widened, but a wider rectangular notch tends to raise sidelobes and may create paired-echo ghosts. A fixed apodized notch with smooth, tapered edges reduces these sidelobes [5], yet a single taper shape cannot match emitters of different bandwidth — it may over-notch a narrow emitter (wasting signal) or under-cover a wide one (leaving residual RFI). A separate line of work reduces sidelobes after notching by nonlinear apodization: the Apodized RFI Filtering (ARF) approach [6] uses spatially-variant apodization (SVA) [7] in the image domain. Such methods are effective but nonlinear, which can bias distributed clutter and add image-domain cost.

This study is intentionally incremental, and we try to state plainly what is inherited and what is new. The closest prior work is acknowledged: adaptive least-mean-square and Wiener filtering for low-frequency SAR RFI were studied by Lamont-Smith et al. [8], who reported good suppression and sidelobe behaviour for an adaptive Wiener filter; subband spectral cancellation [9] suppresses SAR NBI by subtracting range sub-band spectra; and bandwidth-matched adaptive notches are common in the global navigation satellite system (GNSS) and communications literature [10, 11]. We do not claim Wiener filtering or apodization as new; rather, the specific contributions of this paper are threefold: (i) a specific per-emitter, parametric, spectrally-matched notch on the SAR raw range spectrum, with a simple detector and gating — in effect an adaptive apodization obtained linearly at the suppression stage; (ii) a robust spectral-peak detector for SAR spectra, where a median/MAD threshold tends to degenerate; and (iii) a like-for-like comparison of a hard notch, a fixed apodized notch, and the proposed notch, using peak sidelobe ratio (PSLR), integrated sidelobe ratio (ISLR), image RFI suppression (RFIsupp), and normalised mean-square error (NMSE).

2. MATERIALS AND METHODOLOGY

2.1. SAR raw signal and NBI model

Consider a point scatterer of complex reflectivity A at closest-approach range R_0 and azimuth position x_0 in a broadside stripmap geometry. With azimuth (slow) time η and platform velocity v, the range is $R(\eta)$:

$$R(\eta) = \sqrt{(R_0^2 + (v\eta - x_0)^2)} \quad (1)$$

Writing the round-trip delay as $t_d(\eta) = 2R(\eta)/c$ (with c the speed of light), the demodulated echo in range (fast) time τ, for a linear-FM chirp of rate K_r, is:

$$s(\tau,\eta) = Aw_r(\tau - t_d)w_a(\eta)e^{j\pi K_r(\tau - t_d)^2}e^{(-j4\pi R/\lambda)} \quad (2)$$

where w_r, w_a are the range and azimuth amplitude envelopes and λ the wavelength. Mitigation is carried out in the range-frequency domain, $X(f,\eta) = \mathcal{F}_\tau\{s\}$, where f is range frequency and $\mathcal{F}_\tau$ is the Fourier transform along τ. The chirp occupies $|f| \le B_r/2$ with chirp bandwidth $B_r = |K_r|T_p$ (T_p the pulse length). NBI is modelled as M finite-bandwidth emitters within the SAR receive band (here X-band, around the carrier frequency f_c), the m-th centred at a range-frequency f_m with a tall core and lower tapered skirts of emitter-specific width, and decorrelated across azimuth. Averaging the contaminated spectrum X_{rfi} over azimuth:

$$P(f) = \left\langle |X_{rfi}(f,\eta)|^2 \right\rangle_\eta \quad (3)$$

2.2. Hard notch and its limitation

A notch applies a real gain $g(f) \in [0,1]$ to each pulse, $\hat{X} = g\,X_{\text{rfi}}$. The hard notch sets $g = 0$ on a stop-band $\mathcal{S}$ and $g = 1$ elsewhere. Its effect on the range impulse response h is

$$\hat{h} = h - h * \psi \quad (4)$$

where $\hat{h}$ is the mitigated response, operator $*$ is convolution, and ψ is the time-domain response of the stop-band (the inverse transform of the band indicator). For a rectangular stop-band of width W, ψ is a slowly decaying sinc, so widening stop-band $\mathcal{S}$ raises sidelobes. A hard notch therefore trades rejection (favouring large W) against sidelobes (favouring small W); a fixed apodized notch softens the edges but still uses one shape for all emitters.

2.3. Robust spectral-peak detection

We remove the signal envelope with a sliding median of length L (taken wider than the emitter bandwidth), $\bar{P}_{\mathrm{dB}} = \mathrm{movmedian}(10\log_{10} P,\, L)$, and define the residual $r(f)$ in decibels. A bin is flagged as interference when it stands clearly above the local baseline and lies in the occupied band:

$$r(f) = 10\log_{10} P(f) - \bar{P}_{dB}(f) \quad (5)$$

$$C = \{ f : r(f) > T_d \ \&\ f_{in-band} \} \quad (6)$$

where T_d is a detection margin (about 8–12 dB) and "in-band" means the baseline is within T_d dB of its maximum. We use an absolute margin rather than a median/MAD (median absolute deviation) threshold because, on SAR spectra, the residual is near zero away from the few emitters, so the MAD tends to collapse and a relative threshold would flag the natural ripple. The set C is used only to locate the emitters; the notch shape itself comes from the gain below.

2.4. Proposed interference-matched notch

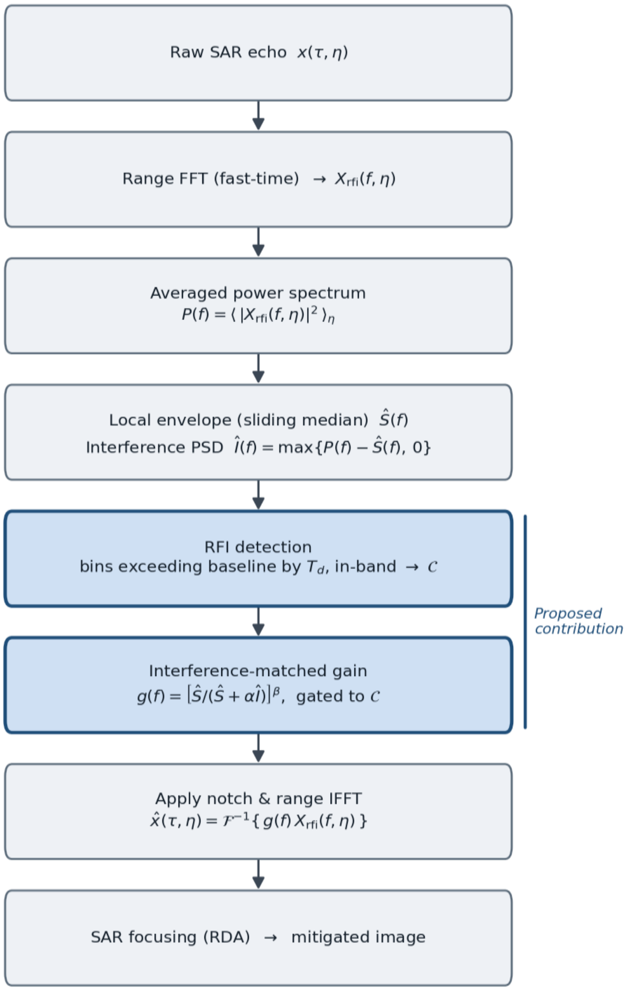

Figure 1. *Block diagram of the proposed interference-matched notch.*

Treating the interference as additive coloured noise, we estimate the signal-plus-noise power spectral density (PSD) by the local envelope, $\hat{S} = 10^{\bar{P}_{\mathrm{dB}}/10}$, and the interference PSD by its excess, $\hat{I} = \max(P - \hat{S},\, 0)$. A parametric Wiener (minimum-mean-square-error, MMSE) gain is then defined as $g(f)$:

$$g(f) = \left[\frac{\hat{S}}{\hat{S} + \alpha \hat{I}} \right]^{\beta} \tag{7}$$

applied near C and set to 1 elsewhere; $\alpha \geq 1$ controls how strongly the cores are suppressed and $\beta \geq 1$ the sharpness of the roll-off. Because g depends on the measured $\hat{I}$, its shape follows each emitter: where interference dominates ($\hat{I} \gg \hat{S}$) the gain approaches 0, so the emitter core is effectively removed — a spectral null, as in any notch; where interference is absent ($\hat{I} \approx 0$) the gain is near 1 and the signal is kept; and in between the gain transitions smoothly along the emitter's measured skirts. The benefit over a rectangular notch is therefore not the avoidance of a spectral null at the core, but the smooth, data-matched transition and the automatic adaptation of the notch width to each emitter: a narrow emitter yields a narrow notch and a wide one a wide, smoothly tapered notch, with no fixed width or taper to set per scene. The cost is about one spectral multiplication per pulse. Figure 1 summarises the pipeline; the two highlighted blocks (detection and matched gain) are the contribution, the others being standard range-frequency processing.

2.5. Simulation setup and compared methods

A broadside stripmap scene (5 point targets and 140 speckle scatterers) is focused with a Range-Doppler algorithm (RDA) focuser [12] using Hamming weighting [13], so the reference impulse-response floor is about −30 dB and notch artefacts are visible. Parameters: carrier frequency f_c = 9.6 GHz, range sampling rate $f_s = 120$ MHz, chirp bandwidth $B_r = 80$ MHz, pulse length T_p = $10\,\mu$s, data size $N_r \times N_a = 1024 \times 512$ (range × azimuth samples), platform velocity $v = 200$ m/s, pulse repetition frequency (PRF) = 1000 Hz, scene-centre range $R_0 = 15$ km, and raw signal-to-noise ratio SNR = 5 dB. Three emitters of different bandwidth (narrow, medium, and wide with heavier skirts) are added at a total interference-to-noise ratio (INR) = 32 dB, so that no single fixed notch width is ideal. The proposed gain uses $\alpha = 1$ (a pure Wiener gain) and $\beta = 2$ (a moderately sharp roll-off); these values are fixed for all experiments and are not tuned per scene. Four cases are compared at a common detection setting: no mitigation; hard notch; fixed apodized notch; and the proposed matched notch. We restrict the comparison to this linear notch family, so that all methods act at the same processing stage and the comparison is like-for-like. A comparison with nonlinear sidelobe-apodization methods such as spatially-variant apodization or Apodized RFI Filtering [6, 7] is left to future work, since a faithful implementation requires a per-pixel optimisation on Nyquist-sampled data and would not be directly comparable to the linear notches here. We report point-target PSLR and ISLR (lower is better), image RFIsupp (higher is better), and NMSE relative to the RFI-free reference (lower is better).

3. RESULTS AND DISCUSSION

Table 1 summarises the quantitative comparison. Among the methods tested, the proposed notch gives the lowest PSLR and ISLR and the smallest NMSE. The remainder of this section examines each result figure in turn.

The table shows one main point. With emitters of different bandwidth, the fixed apodized notch is the weakest at suppressing the RFI — its RFIsupp of 24.6 dB is even slightly below that of the hard notch — because a single taper cannot both cover the wide emitter and spare the narrow one. Matching the shape per emitter recovers RFIsupp to 28.4 dB and, at the same time, gives the lowest PSLR, ISLR, and NMSE among the three notches. The improvement is modest but consistent across the metrics, and is obtained at essentially the cost of a hard notch.

Table 1. *Heterogeneous-NBI comparison with fixed random seed.*

Method	RFI suppression (dB)	PSLR (dB)	ISLR (dB)	NMSE (dB)
No mitigation	0.0	−13.25	−3.21	−0.15
Hard notch	27.3	−13.58	−6.12	−6.05
Apodized (fixed)	24.6	−14.92	−7.05	−6.05
Matched notch (proposed)	28.4	**−15.11**	**−7.24**	**−7.03**
RFI-free reference	—	−30.03	−25.28	—

Figure 2 shows the averaged range-frequency spectrum (top) and the notch gains (bottom). The three emitters of different bandwidth appear as peaks of different width on the smooth signal envelope. The hard notch (black) is a fixed rectangular stop and the fixed apodized notch (blue) is a fixed tapered one; both apply the same shape to every emitter. The proposed gain (orange) instead follows each peak — narrow and sharp at the narrow emitter, wide and smoothly tapered at the wide one — obtained directly from the measured spectrum, with no width or taper to set by hand.

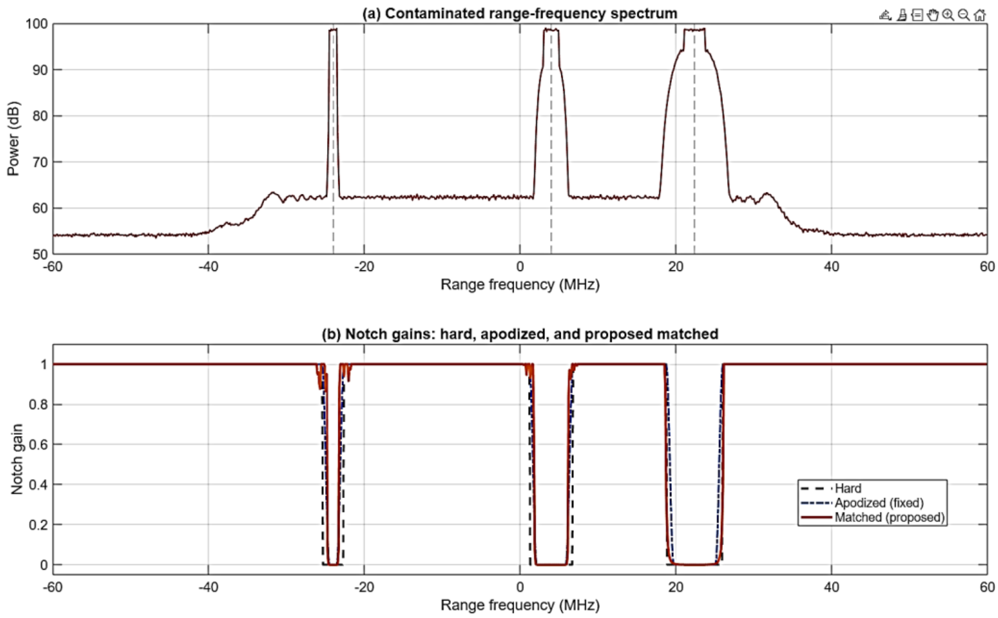

Figure 2. *(a) Averaged range-frequency spectrum (three emitters of differing bandwidth); (b) hard, fixed-apodized, and proposed matched-notch gains.*

Figure 3 shows the range impulse response of an isolated point target for the four cases. Without mitigation the interference raises the whole sidelobe region; the three notches lower it, and the proposed notch (drawn in bold) has the lowest peak and integrated sidelobes (Table 1). Every notch here leaves a sidelobe floor well above the RFI-free reference (about −15 dB versus −30 dB): removing a band of frequencies punches holes in the spectrum, and the Hamming weighting only controls the sidelobes caused by band-edge truncation, not those caused by interior holes. To confirm that this is a property of the notch rather than an artefact of the implementation, we applied the same gain $g(f)$ to a *clean* point target (no interference): the PSLR fell from −31.6 dB to −15.0 dB although no RFI was present, the Hamming weights were unchanged outside the notch (deviation $< 10^{-3}$), and removing the Hamming weighting made the PSLR worse (-12.4 dB), which shows the window is still active and that the loss comes from the spectral holes alone. The residual level reflects the notched fraction of the band (here about 11%, as the three emitters are deliberately wide and strong), so the comparison between methods is relative, at a common operating point, rather than a claim of near-ideal sidelobes.

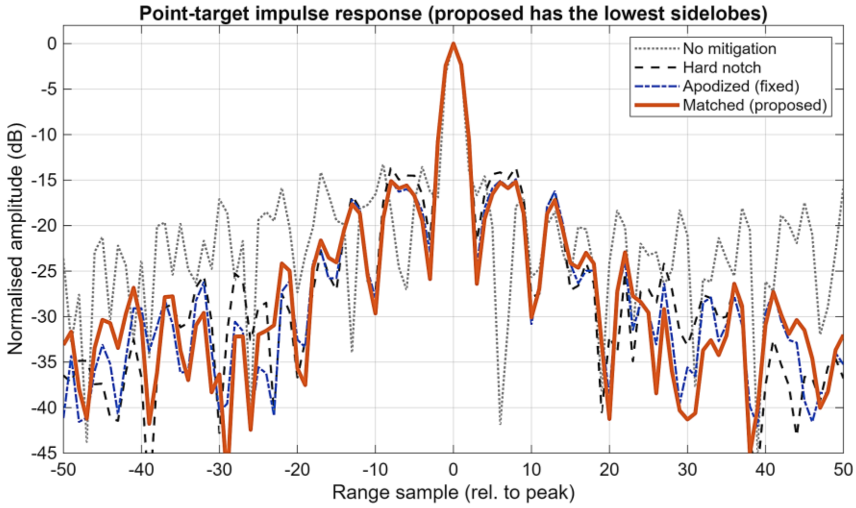

Figure 3. *Isolated point-target range impulse response; the matched notch keeps the sidelobes a little below the hard and fixed-apodized responses.*

Figure 4 sweeps the notch width for the hard and fixed apodized notches, plotting PSLR and RFI suppression against the notched fraction of the band, and overlays the proposed matched notch as a star. The sweep makes the underlying trade-off explicit: widening the notch improves RFI suppression but raises the sidelobes. The proposed notch sits off these curves — it reaches a high RFI suppression at a small notched fraction (about 11%), which the hard and apodized notches attain only at a larger width and hence higher sidelobes. This is the practical benefit of adapting the width to each emitter rather than choosing one global width.

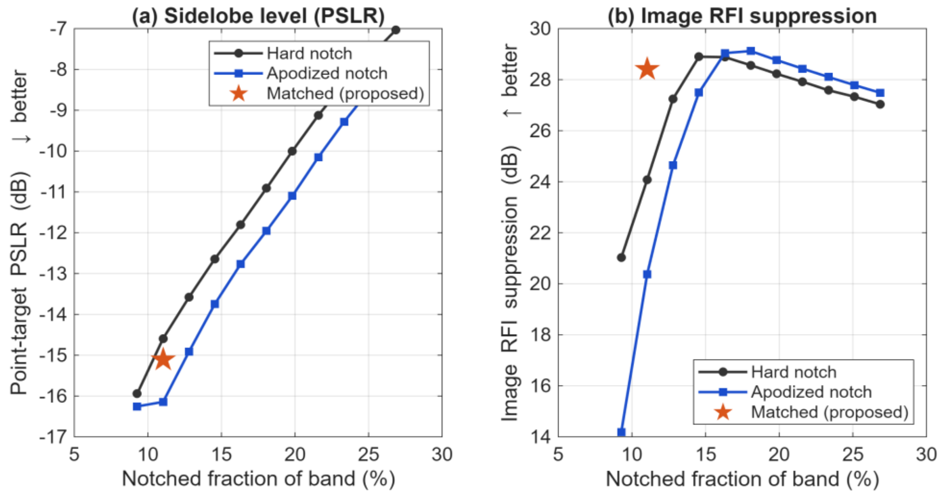

Figure 4. *Notch-width sweep for hard and fixed apodized filters: PSLR and RFI suppression versus the notched fraction.*

Figure 5 summarises Table 1 as bar charts of the four metrics, with the RFI-free reference indicated for PSLR and ISLR. The proposed notch is best (or tied) on all four; the margin over the fixed apodized notch is clearest for RFI suppression and NMSE.

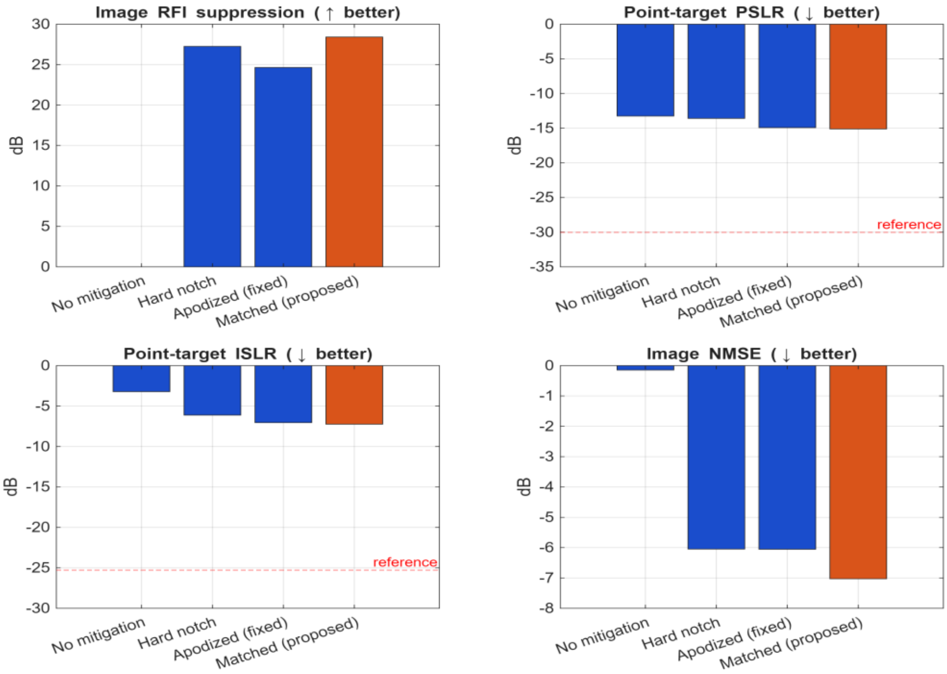

Figure 5. *Bar summary of Table 1: image RFI suppression, point-target PSLR and ISLR, and image NMSE.*

4. CONCLUSIONS

In this paper, we presented a simple, low-complexity notch filter for narrowband-RFI suppression in SAR. By estimating the interference spectrum of each emitter and applying a parametric Wiener gain, the notch adjusts its width and roll-off to the emitter, which helps ease the hard notch's trade-off between rejection and sidelobes without a fixed taper or nonlinear post-processing. On a 2-D SAR simulation with emitters of differing bandwidth, it gave favourable PSLR (about −15.1 dB), ISLR (about −7.2 dB), and NMSE (about −7.0 dB) among the compared methods, while remaining linear and at roughly hard-notch cost. The work is incremental: the inherited Wiener/apodization ideas are attributed to prior work, and the per-emitter matched design and comparison are the contribution. Future work will study the choice of (α, β), a two-dimensional (range–azimuth) extension, and validation on real Sentinel-1 Level-0 data with various RFI types.

REFERENCES

[1]. M. Tao, J. Su, Y. Huang, and L. Wang, "*Mitigation of radio frequency interference in synthetic aperture radar data: Current status and future trends*", Remote Sensing, vol. 11, no. 20, Art. no. 2438, (2019). DOI: 10.3390/rs11202438

[2]. F. Zhou, R. Wu, M. Xing, and Z. Bao, "*Eigensubspace-based filtering with application in narrow-band interference suppression for SAR*", IEEE Geoscience and Remote Sensing Letters, vol. 4, no. 1, pp. 75–79, (2007). DOI: 10.1109/LGRS.2006.887033

[3]. M. Tao, F. Zhou, J. Liu, Y. Liu, Z. Zhang, and Z. Bao, "*Narrow-band interference mitigation for SAR using independent subspace analysis*", IEEE Transactions on Geoscience and Remote Sensing, vol. 52, no. 9, pp. 5289–5301, (2014). DOI: 10.1109/TGRS.2013.2287900

[4]. Y. Ding, W. Fan, Z. Zhang, F. Zhou, and B. Lu, "*Radio frequency interference mitigation for synthetic aperture radar based on the time-frequency constraint joint low-rank and sparsity properties*", Remote Sensing, vol. 14, no. 3, Art. no. 775, (2022). DOI: 10.3390/rs14030775

[5]. W. Chang, J. Li, and X. Li, "*The effect of notch filter on RFI suppression*", Wireless Sensor Network, vol. 1, no. 3, pp. 196–205, (2009). DOI: 10.4236/wsn.2009.13026

[6]. A. W. Doerry, "*Apodized RFI filtering of synthetic aperture radar images*", Sandia National Laboratories, Albuquerque, NM, USA, Sandia Report SAND2014-1376, (2014). DOI: 10.2172/1204095

[7]. H. C. Stankwitz, R. J. Dallaire, and J. R. Fienup, "*Nonlinear apodization for sidelobe control in SAR imagery*", IEEE Transactions on Aerospace and Electronic Systems, vol. 31, no. 1, pp. 267–279, (1995). DOI: 10.1109/7.366309

[8]. T. Lamont-Smith, R. D. Hill, S. D. Hayward, G. Yates, and A. P. Blake, "*Filtering approaches for interference suppression in low-frequency SAR*", IEE Proceedings - Radar, Sonar and Navigation, vol. 153, no. 4, pp. 338–344, (2006). DOI: 10.1049/ip-rsn:20050092

[9]. J. Feng, H. Zheng, Y. Deng, and D. Gao, "*Application of subband spectral cancellation for SAR narrow-band interference suppression*", IEEE Geoscience and Remote Sensing Letters, vol. 9, no. 2, pp. 190–193, (2012). DOI: 10.1109/LGRS.2011.2163150

[10]. T. T.-T. Nguyen, V. L. The, T. H. Ta, H.-L. T. Nguyen, and B. Motella, "*An adaptive bandwidth notch filter for GNSS narrowband interference mitigation*", REV Journal on Electronics and Communications, vol. 4, no. 3–4, pp. 59–68, (2014). DOI: 10.21553/rev-jec.76

[11]. M. H. Same, G. Gleeton, G. Gandubert, P. Ivanov, and R. Landry, "*Multiple narrowband interferences characterization, detection and mitigation using simplified Welch algorithm and notch filtering*", Applied Sciences, vol. 11, no. 3, Art. no. 1331, (2021). DOI: 10.3390/app11031331

[12]. I. G. Cumming and F. H. Wong, "*Digital Processing of Synthetic Aperture Radar Data: Algorithms and Implementation*", Norwood, MA, USA: Artech House, (2005).

[13]. F. J. Harris, "*On the use of windows for harmonic analysis with the discrete Fourier transform*", Proceedings of the IEEE, vol. 66, no. 1, pp. 51–83, (1978). DOI: 10.1109/PROC.1978.10837

[14]. W. Xu, W. Xing, C. Fang, P. Huang, and W. Tan, "*RFI suppression based on linear prediction in synthetic aperture radar data*", IEEE Geoscience and Remote Sensing Letters, vol. 18, no. 12, pp. 2127–2131, (2021). DOI: 10.1109/LGRS.2020.3015205

[15]. Z. Wang, W. Yu, J. Li, Z. Yu, Y. Zhao, and Y. Luo, "*Radio frequency interference mitigation in synthetic aperture radar data based on instantaneous spectrum forward consecutive mean excision*", Remote Sensing, vol. 16, no. 1, Art. no. 150, (2024). DOI: 10.3390/rs16010150

[16]. D. T. Nguyen, "*Segmentation and reconstruction of wireless signals under interference using the FoT-UNet neural network*", Journal of Military Science and Technology, vol. 110, pp. 45–54, (2026). DOI: 10.54939/1859-1043.j.mst.110.2026.45-54

TÓM TẮT

Bộ lọc notch khớp phổ nhiễu để chế áp nhiễu tần số vô tuyến dải hẹp trong ra đa khẩu độ tổng hợp

Nhiễu tần số vô tuyến dải hẹp (NBI) làm suy giảm chất lượng ảnh ra đa khẩu độ tổng hợp (SAR). Lọc notch trong miền tần số là giải pháp phổ biến, nhưng bộ lọc notch cứng (dạng chữ nhật) vướng sự đánh đổi giữa chế áp nhiễu và búp phụ, còn bộ lọc notch vát mép với tham số cố định không phù hợp với các nguồn nhiễu có độ rộng băng khác nhau. Bài báo đề xuất một bộ lọc notch đơn giản, độ phức tạp thấp, có hình dạng khớp theo phổ nhiễu đo được. Dựa trên ý tưởng lọc Wiener cổ điển, bộ lọc ước lượng mật độ phổ công suất của từng nguồn nhiễu từ phổ cự ly trung bình của SAR rồi áp một hàm khuếch đại sai số trung bình bình phương cực tiểu có tham số, với phần vát mép bám theo dạng phổ của nguồn nhiễu đó; bộ lọc tuyến tính, không cần tinh chỉnh theo từng cảnh và chỉ tốn khoảng một phép nhân phổ trên mỗi xung. Trên mô phỏng SAR 2-D với các nguồn nhiễu có độ rộng băng khác nhau, phương pháp cho tỷ số búp phụ tại đỉnh (PSLR) khoảng −15,1 dB, tỷ số búp phụ tích hợp (ISLR) khoảng −7,2 dB và sai số bình phương trung bình chuẩn hóa (NMSE) nhỏ nhất, khoảng −7,0 dB, so với bộ lọc notch cứng và bộ lọc notch vát mép cố định. Đóng góp của bài báo là thiết kế bộ lọc notch khớp phổ theo từng nguồn nhiễu và đánh giá so sánh hiệu quả của giải pháp đề xuất với các hướng tiếp cận khác.

Từ khoá: Ra đa khẩu độ tổng hợp; Xử lý tín hiệu số ra đa; Chế áp nhiễu tần số vô tuyến; Nhiễu tần số vô tuyến dải hẹp; Bộ lọc notch.